



Mass and Energy Preservation of Mimetic Difference Schemes for General Systems of Conservation Laws

Miguel A. Dumett and Jose E. Castillo

June 23, 2024

Publication Number: CSRCR2024-06

Computational Science &
Engineering Faculty and Students
Research Articles

Database Powered by the
Computational Science Research Center
Computing Group & Visualization Lab

COMPUTATIONAL SCIENCE & ENGINEERING



**SAN DIEGO STATE
UNIVERSITY**

Computational Science Research Center
College of Sciences
5500 Campanile Drive
San Diego, CA 92182-1245
(619) 594-3430



Mass and Energy Preservation of Mimetic Difference Schemes for General Systems of Conservation Laws ^{*}

Miguel A. Dumett [†] Jose E. Castillo¹

June 23, 2024

Abstract

In this paper, mass and energy preservation of high-order mimetic difference schemes for general systems of conservation laws is mathematically demonstrated. The proof of mass preservation is based on the relationship between the divergence discrete analog and the associated quadrature of the generalized inner product weights which satisfy the integration by parts formula. The proofs begin with the one-dimensional scalar case, the one-dimensional general case, and ends with the system of conservation laws in any dimension. The energy preservation proofs follow the same pattern. Nevertheless, the general case for the energy preservation requires a different approach, one based on the application of several times the one-dimensional quadrature property of the inner weights for the gradient and divergence. Furthermore, numerical validation of this conservation is provided by some numerical examples.

1 Introduction

System of conservation laws postulate the balance of certain quantities (conservation) in certain volumes by considering fluxes entering/exiting the boundary of the domain.

These systems of c partial differential equations (conservation laws) are described by

$$\begin{aligned} \frac{\partial u}{\partial t} + \nabla \cdot f(u, x, t) &= 0, & x \in \Omega, t > 0, \\ u(x, 0) &= g, & x \in \Omega, \end{aligned}$$

for $\Omega \subset \mathbb{R}^d$, a region in the d -dimensional space.

For scalar one-dimensional conservation laws, one can show by utilizing the method of characteristics, that in general there does not exist a smooth solution for all $t > 0$, but

^{*}This work was partially supported by SDSU.

[†]Computational Science Research Center at the San Diego State University.

locally. For systems of conservation laws, there is no a complete mathematical understanding of the solutions in higher dimensions than one. In general, one needs to consider weak solutions. In the case of discontinuous initial data, the Rankine-Hugoniot condition is required to extend the solution further away the local neighborhood obtained by the method of characteristics. However, for uniqueness one needs the Entropy condition, and the Lax-Oleinik formula that describes it [13]. In the case of semilinear systems in non-divergence form, it is possible to find global solutions in the form of traveling waves for strictly hyperbolic systems. In the case of 1D nonlinear systems of conservation laws, one can find conditions for the existence of local solutions composed of rarefaction and shock waves [13]. We assume solutions of the systems of conservation laws that are smooth.

Different methods have been utilized for numerically solving systems of conservation laws. Among them finite differences, finite volume, and some monotone and flux limited schemes. For higher-order methods, avoiding the oscillations produced when one of the previous method was utilized to obtain high-order accurate solutions, leads to essentially non-oscillatory (ENO) schemes and later to weighted essentially non-oscillatory (WENO) methods. The complexity of the computational grid structure involved in ENO and WENO triggered the evolution towards discontinuous Galerkin methods, in the sense that ENO schemes expressed in the volume form, do allow the usage of non-uniform and fully unstructured grids, although the computational cost remains high [14]. Since we focus on smooth solutions, we do not have to deal with these situations.

Mimetic methods attempt to mimic properties of the solutions such as symmetries, conservation laws, fundamental identities and/or some integral vector calculus identities and with that aim they try two different approaches: traditionally, they construct vector calculus differential operator discrete analogs enforcing high-order accurate approximations of integral identities (among them [21, 3, 4, 5]), or more recently, their goal is to replicate a discrete version of the vector, and/or tensor, and/or exterior calculi (for example [19, 2, 17, 15, 16]), algebraic topology structures (as in [11, 12]), or geometric and structure-preserving methods [20], and the references therein.

One mimetic technique that is not computationally expensive is the one given by the mimetic differences (MD) developed originally by [3] and efficiently improved by [4]. They belong to the first group. They satisfy the integration by parts (IBP) formula in one-dimension (1D), and later via interpolation operators [6], the three-dimensional (3D) analogue or extended Gauss' divergence theorem. These approaches introduce independently discrete analogs D and G of the divergence and gradient first-order differential operators. These operators achieve uniform accuracy over the whole domain, including grid points near and at the boundary. This is a unique feature of MD not only among any other mimetic approach but also among any spatial discretization method in general. Moreover, it achieve a high-order approximation of the discrete analog of the IBP formula, with the weighted inner product Q and P for integral with divergence and gradient integrands [3, 4].

It turns out that these weights are bonafide high-order quadratures [1] on its own. Additionally, it has been demonstrated that MD operators verify vector calculus identities [8], and that MD schemes conserve energy for the advection equation [7, 9].

This paper targets at proving that MD schemes preserve mass and energy for systems of c conservation laws in d dimensions. This is exhibited by some numerical examples.

The rest of the paper is organized in the following way. In Section 2, the systems of nonlinear conservation laws with boundary and initial conditions are described. In Section 3 mimetic difference and its major analog operator properties for any number of dimensions are stated. In Section 4, mass preservation of MD schemes established for the one-dimensional (1D) scalar and system cases, as well as for the general system in any number of dimensions. In Section 5, a similar pattern is utilized for demonstrating the preservation of energy of mimetic schemes for general systems of conservation laws. In Section 6, numerical validation is shown via several examples. In Section 7 conclusions of this work are drawn.

2 Systems of conservation laws

Even though this paper consider systems of conservation laws in general, some specific geometry and associated boundary conditions are given to facilitate the proofs of mass and energy preservation.

Given the following sets

$$I = \{1, \dots, c\}, \quad J = \{1, \dots, d\}, \quad L = [-1, 1]^d, \quad L_0 = [-1, 1]^{d-1}, \quad K = [0, T],$$

consider the system of c conservation laws in d -dimensions, with $x = (x_1, \dots, x_d)$, and the unknown $u(x, t) = (u_1(x, t), \dots, u_c(x, t))^T$, and initial condition $u^0(x) = (u_1^0(x), \dots, u_c^0(x))^T$, that are described by

$$u_t + \operatorname{div}(F(u)) = 0_{c \times 1}, \quad (x, t) \in \mathring{L} \times \mathring{K}, \quad (1)$$

$$u(x, 0) = u^0(x), \quad x \in L, \quad (2)$$

with $\mathring{L} = \operatorname{int}(L)$, the interior of L , and that hold boundary conditions given by

$$u_i(x_1, \dots, x_{j-1}, -1, x_{j+1}, \dots, x_d, t) = g_i^-(x_1, \dots, x_{j-1}, x_{j+1}, \dots, x_d, t), \quad i \in I, j \in J,$$

$$u_i(x_1, \dots, x_{j-1}, 1, x_{j+1}, \dots, x_d, t) = g_i^+(x_1, \dots, x_{i-1}, x_{i+1}, \dots, x_d, t), \quad i \in I, j \in J,$$

where $g_i^\pm : L_0 \times K \rightarrow \mathbb{R}^c$, $i = 1, \dots, c$, are smooth functions. The flux F is given by

$$F(u) = \begin{pmatrix} F_{11}(u) & \cdots & F_{1d}(u) \\ \vdots & \ddots & \vdots \\ F_{c1}(u) & \cdots & F_{cd}(u) \end{pmatrix}.$$

Notice $F_{ij} : \mathbb{R}^d \times \mathring{K} \rightarrow \mathbb{R}$, $i \in I, j \in J$. Denote $F_i(u) = (F_{i1}(u), \dots, F_{id}(u))^T$, $i \in I$.

3 Mimetic differences

In this section, we present a summary of mimetic difference operators in 1D and in general d -dimensions and their major properties and relationships.

3.1 Some mimetic difference operator properties in 1D

In $[-1, 1]$, MD utilizes a mesh of N uniform cells and a staggered grid. The staggered grid is composed of a face grid that contains the edges of the cells (or nodes)

$$X_F = \left\{ x_l = -1 + \frac{2l}{N}, 0 \leq l \leq N \right\},$$

and a center grid, that includes all center cells and domain boundary points,

$$X_C = \{-1\} \cup \left\{ x_{l+\frac{1}{2}} = -1 + \frac{1}{N} + \frac{2l}{N}, 0 \leq l \leq N-1 \right\} \cup \{1\}.$$

In MD, it is traditionally assumed that scalar fields are defined at X_C , and vector fields are defined at X_F . In general, where the data is located and where the space partial derivative is calculated is not essential, since there exist mimetic high-order interpolation operators from X_C to X_F and vice-versa [6]. Nevertheless, suppose data is located following the classic assumption. That said, the discrete version of the components of the unknown u , given by U , take values on X_C . Furthermore, presume that each of the components of the flux takes values on centers and vertices and return values on centers and vertices.

The MD discrete analog of the divergence operator D has a non-square matrix representation $D : X_N \rightarrow X_C$. In addition, it presumes that the discrete analog of the gradient operator is a transformation $G : X_C \rightarrow X_N$. The condition that D and G of discrete constant fields should be zero impose the zero row sum constraint on both.

Moreover, MD operators are chiefly constructed to approximate with high accuracy the integration by parts formula (IBP) for 1D scalar field f and 1D vector field \vec{v} ,

$$\int_U \vec{v} \cdot \nabla f \, dU + \int_U f \nabla \cdot \vec{v} \, dU = \int_{\partial U} f \vec{v} \cdot \vec{n} \, dS. \quad (3)$$

For achieving this, it is required to use Q, P positive diagonal matrix weights that define generalized inner products and the mimetic discrete analog is defined as

$$\Delta x \langle DV, F \rangle_Q + \Delta x \langle V, GF \rangle_P = V_N F_N - V_0 F_0. \quad (4)$$

where F, V are the projections of f, \vec{v} to X_C, X_N , respectively. It can be shown that both Q and P exist and that define high-order quadratures for any smooth functions [1].

When considering the constant discrete scalar field $F \equiv 1$ in (4), it follows that

$$(\Delta x) D^T Q \mathbf{1} = (-1, 0, \dots, 0, 1)^T \in \mathbb{R}^{N+2}. \quad (5)$$

3.2 Some mimetic difference operator properties in d -dimensions

In $[-1, 1]^d$, MD utilizes m_l cells along axis X_l , $l = 1, \dots, d$. The staggered grid is composed of cell centers and cell vertices X_C , and of cell centered faces X_F , given respectively by

$$\begin{aligned} X_F &= \bigcup_{j=1}^d \left[\left(\prod_{l < j} (X_C^j \setminus \{-1, 1\}) \right) \times X_F^j \times \left(\prod_{l > j} (X_C^j \setminus \{-1, 1\}) \right) \right], \\ X_C &= \prod_{j=1}^d X_C^j. \end{aligned}$$

Extensions of the 1D divergence D , gradient G , and inner product weight operators Q and P are built by utilizing Kronecker products of the 1D operators and some near identity of convenient orders. So, one has that the matrix representations of:

1. The discrete analogs of the order k divergence $D_{x_1, \dots, x_d} : X_C \rightarrow X_F$, is

$$\begin{aligned} D_{x_1, \dots, x_d}^{(k)} &= [D_{x_1, \dots, x_d, 1}^{(k)}, \dots, D_{x_1, \dots, x_d, d}^{(k)}] \\ &= [\hat{I}_{m_d} \otimes \dots \otimes \hat{I}_{m_2} \otimes D_{x_1}^{(k)}, \dots, D_{x_d}^{(k)} \otimes \hat{I}_{m_{d-1}} \otimes \dots \otimes \hat{I}_{m_1}], \end{aligned}$$

where $D_{x_p}^{(k)}$ is the 1D divergence operator of accuracy order k along the p -axis, and

$$\hat{I}_q = \begin{bmatrix} 0_{1 \times q} \\ I_{q \times q} \\ 0_{1 \times q} \end{bmatrix},$$

with $I_{q \times q}$ is the $q \times q$ identity matrix.

2. The discrete analogs of the order k gradient $G_{x_1, \dots, x_d} : X_C \rightarrow X_F$,

$$G_{x_1, \dots, x_d}^{(k)} = \begin{bmatrix} G_{x_1, \dots, x_d, 1}^{(k)} \\ \vdots \\ G_{x_1, \dots, x_d, d}^{(k)} \end{bmatrix} = \begin{bmatrix} \hat{I}_{m_d}^T \otimes \dots \otimes \hat{I}_{m_2}^T \otimes G_{x_1}^{(k)} \\ \vdots \\ G_{x_d}^{(k)} \otimes \hat{I}_{m_{d-1}}^T \otimes \dots \otimes \hat{I}_{m_1}^T \end{bmatrix},$$

where $G_{x_p}^{(k)}$ is the 1D gradient operator of accuracy order k along the p -axis.

3. The mimetic discrete inner product weight operators $Q_{x_1, \dots, x_d} \in \mathbb{R}^{|X_C| \times |X_C|}$, where $|X_C| = \prod_{j=1}^d (m_j + 2)$, is the cardinality of X_C ,

$$Q_{x_1, \dots, x_d}^{(k)} = \begin{bmatrix} I_{m_d+2} \otimes \cdots \otimes I_{m_2+2} \otimes Q_{m_1+2}^{(k)} & & \\ & \ddots & \\ & & Q_{m_d+2}^{(k)} \otimes I_{m_{d-1}+2} \otimes \cdots \otimes I_{m_1+2} \end{bmatrix},$$

where $Q_m^{(k)} \in \mathbb{R}^{m \times m}$ is the 1D inner product weight Q of accuracy order k .

4. The mimetic discrete inner product weight operators $P_{x_1, \dots, x_d} \in \mathbb{R}^{|X_F| \times |X_F|}$, where $|X_F| = \sum_{j=1}^d (m_j + 1) \prod_{l \neq j} m_l$, is the cardinality of X_F ,

$$P_{x_1, \dots, x_d}^{(k)} = \begin{bmatrix} I_{m_d+2} \otimes \cdots \otimes I_{m_2+2} \otimes P_{m_1+1}^{(k)} & & \\ & \ddots & \\ & & P_{m_d+1}^{(k)} \otimes I_{m_{d-1}+2} \otimes \cdots \otimes I_{m_1+2} \end{bmatrix},$$

where $P_m^{(k)} \in \mathbb{R}^{m \times m}$ is the 1D inner product weight P of accuracy order k .

In d -dimensions, $d > 1$, there are different partial derivatives. For the gradient, each of them is approximated at exactly one of the faces of the hyper-cube $[-1, 1]^d$. Similarly, for the divergence, each component takes its input from a different face of $[-1, 1]^d$. Since scalar fields defined on $[-1, 1]^d$ are defined at centers, then different quantities may be at different set of points making difficult to compute their product in the extension of the integration by part formula in d -dimensions. High-order interpolation to move the data from one set of points to another are needed.

The d -dimension versions of them are defined also by Kronecker products between the corresponding 1D interpolation version and some identity matrices. They are given by

1. Interpolations from X_C to X_F given by

$$\begin{aligned} (I^D)_{x_1, \dots, x_d}^{(k)} &= \begin{bmatrix} (I^D)_{x_1, \dots, x_d, 1}^{(k)} & & \\ & \ddots & \\ & & (I^D)_{x_1, \dots, x_d, d}^{(k)} \end{bmatrix} \\ &= \begin{bmatrix} \hat{I}_{m_d}^T \otimes \cdots \otimes \hat{I}_{m_2}^T \otimes (I^D)_{x_1}^{(k)} & & \\ & \ddots & \\ & & (I^D)_{x_d}^{(k)} \otimes \hat{I}_{m_{d-1}}^T \otimes \cdots \otimes \hat{I}_{m_1}^T \end{bmatrix}, \end{aligned}$$

where $(I^D)_{x_p}^{(k)}$ is the 1D interpolation operator from X_C^p to X_F^p of accuracy order k along the p -axis.

2. Interpolations from X_F to X_C given by

$$\begin{aligned} (I^G)_{x_1, \dots, x_d}^{(k)} &= \begin{bmatrix} (I^G)_{x_1, \dots, x_d, 1}^{(k)} & & & \\ & \ddots & & \\ & & (I^G)_{x_1, \dots, x_d, d}^{(k)} & \\ & & & \end{bmatrix} \\ &= \begin{bmatrix} \hat{I}_{m_d} \otimes \dots \otimes \hat{I}_{m_2} \otimes (I^G)_{x_1}^{(k)} & & & \\ & \ddots & & \\ & & & (I^G)_{x_d}^{(k)} \otimes \hat{I}_{m_{d-1}} \otimes \dots \otimes \hat{I}_{m_1} \end{bmatrix}, \end{aligned}$$

where $(I^G)_p^{(k)}$ is the 1D interpolation operator from X_F^p to X_C^p of accuracy k along the p -axis.

The extension of the 1D integration by parts formula to d -dimension is called the extended Gauss divergence theorem. The discrete analog of the extended Gauss divergence theorem, neglecting the order of accuracy k , reads

$$\left(\prod_{l=1}^d \Delta x_l \right) \langle P_{x_1, \dots, x_d} G_{x_1, \dots, x_d} F, \vec{V} \rangle + \left(\prod_{l=1}^d \Delta x_l \right) \langle Q_{x_1, \dots, x_d} F, D_{x_1, \dots, x_d} \vec{V} \rangle = F^T \bar{B}_{x_1, \dots, x_d} \vec{V},$$

where F is the projection onto X_C of scalar field $f : \mathbb{R}^d \rightarrow \mathbb{R}$, \vec{V} is the projection onto X_F of vector field $\vec{v} : \mathbb{R}^d \rightarrow \mathbb{R}^d$, and boundary operator

$$\bar{B}_{x_1, \dots, x_d} = \begin{pmatrix} I_{m_d+2} \otimes \dots \otimes I_{m_2+2} \otimes \bar{B}_{x_1} & & & \\ & \ddots & & \\ & & & \bar{B}_{x_d} \otimes I_{m_{d-1}+2} \otimes \dots \otimes I_{m_1+2} \end{pmatrix},$$

where \bar{B}_{x_p} is the one dimensional boundary

$$\bar{B}_{x_p} = \begin{pmatrix} -1 & 0 & \dots & 0 & 0 \\ 0 & 0 & \dots & 0 & 0 \\ \vdots & \vdots & \vdots & \vdots & \vdots \\ 0 & 0 & \dots & 0 & 0 \\ 0 & 0 & \dots & 0 & 1 \end{pmatrix},$$

matrix along the p -axis. It can be proven by a direct computation (see [9, pp. 11-13]) that for a discrete constant scalar field F , one obtains

$$\left(\prod_{l=1}^d \Delta x_l \right) D_{x_1, \dots, x_d}^T Q_{x_1, \dots, x_d} \mathbf{1} = \begin{pmatrix} \mathbf{1} \otimes \mathbf{1} \otimes b_{m_1+1} & & & \\ & \ddots & & \\ & & & b_{m_d+1} \otimes \mathbf{1} \otimes \mathbf{1} \end{pmatrix}, \quad (6)$$

with $b_m = [-1, 0, \dots, 0, 1] \in \mathbb{R}^m$.

4 Mimetic schemes mass preservation for conservation laws

In this section, mass preservation for conservation laws is established. First, the 1D scalar case is treated, then the 1D system of conservation laws, and lastly the general case. For mass preservation of the mimetic scheme, we understand that its numerical solution should verify a discrete analog of the integral form of the scalar conservation law

$$\int_L u(x, T) dx - \int_L u(x, 0) dx = - \int_0^T \int_{\partial L} \vec{n} \cdot f(u, x, t) dS dt, \quad (7)$$

or in the 1D case

$$\int_L u(x, T) dx - \int_L u(x, 0) dx = - \int_0^T (F(u(1, t)) - F(u(-1, t))) dt. \quad (8)$$

4.1 One-dimensional scalar conservation law ($c = 1, d = 1$)

The equation is

$$\begin{aligned} u_t + (F(u))_x &= 0, & x \in (-1, 1), & t \in (0, T), \\ u(x, 0) &= u^0(x), & x \in [-1, 1], \\ u(-1, t) &= g^-(t), & t \in [0, T], \\ u(1, t) &= g^+(t), & t \in [0, T]. \end{aligned} \quad (9)$$

In finite differences, one assumes a uniform mesh in space, with N cells, and M constant time steps (in addition to the step zero where the initial data is), defined on $[-1, 1] \times [0, T]$. The space mesh size is given by $\Delta x = \frac{2}{N}$, and the time step size by $\Delta t = \frac{T}{M}$. To prove mass preservation, usually a discrete scheme for the conservation law is proposed and after a discrete integration in space followed by a discrete integration in time, one makes $\Delta x, \Delta t \rightarrow 0$, and finds that the scheme converges to (8), the integral form of (9). Notice that in this approach, u on the continuum is projected on the computational grid as U at nodes and the divergence is approximated by fluxes computed at cell centers but utilizing data from some nodes.

4.1.1 Mimetic difference scheme of the conservation law

The partial differential equation of the 1D scalar conservation law is given by

$$u_t = -(F(u))_x.$$

If $U^m = (U_0^m, \dots, U_N^m)$, for the m -th time step, with $U_n^m, n \in J$ values taken at the nodes X_C , and if one utilizes forward Euler as a time discretization for u_t , then the mimetic scheme is given by

$$\frac{1}{\Delta t} (U^{m+1} - U^m) = -DI^D F(U^m),$$

where I^D is the mimetic interpolation operator from centers to nodes.

Multiplying by $\mathbf{1}^T Q$ on the left, where Q is the mimetic quadrature weight positive diagonal operator for the divergence and $\mathbf{1}$ is a vector of ones, one gets from (5)

$$\begin{aligned} \frac{1}{\Delta t} \mathbf{1}^T Q(U^{m+1} - U^m) &= -(\mathbf{1}^T Q D) I^D F(U^m) = -\frac{1}{\Delta x} (-1, 0, \dots, 0, 1) I^D F(U^m) \\ &= -\frac{1}{\Delta x} I^D (F(u(1, t_m)) - F(u(-1, t_m))). \end{aligned} \quad (10)$$

This reflects conservation at the discrete level, provided U^0 is defined such

$$(\Delta x) \mathbf{1}^T Q U^0 \approx \int_{-1}^1 u^0(x) dx,$$

which is known to hold for the high-order quadrature Q [1]. Notice that, the term on the left of

$$\Delta x \mathbf{1}^T Q(U^{m+1} - U^m) = -\Delta t I^D (F(u(1, t_m)) - F(u(-1, t_m))),$$

is a high-order approximation of integral $\int_{-1}^1 (U^{m+1}(x) - U^m(x)) dx$.

4.1.2 Mass conservation for periodic boundary conditions

Suppose $Q = \text{diag}(w_n) \in \mathbb{R}^{(N+2) \times (N+2)}$.

Under periodic boundary conditions, (10) becomes

$$\Delta x \sum_{n=0}^N w_n U_n^{m+1} = \Delta x \sum_{n=0}^N w_n U_n^m = \dots = \Delta x \sum_{n=0}^N w_n U_n^0,$$

and this reflects the conservation at the discrete level, since $\Delta x \sum_{n=0}^N w_n U_n^0$ is a high-order approximation of $\int_{-1}^1 u_0(x) dx$.

4.1.3 Mass conservation for non-periodic boundary conditions

In this case, one can sum (10) from $m = 0$ to $m = M$ to obtain

$$(\Delta x) \sum_{m=0}^M \sum_{n=0}^N w_n (U_n^{m+1} - U_n^m) = -(\Delta t) I^D \left[\sum_{m=0}^M F(U(1, t_m)) - \sum_{m=0}^M F(U(-1, t_m)) \right],$$

and by the telescoping property one has

$$\sum_{m=0}^M \sum_{n=0}^N w_n (U_n^{m+1} - U_n^m) = \sum_{n=0}^N w_n \left(\sum_{m=0}^M (U_n^{m+1} - U_n^m) \right) = \sum_{n=0}^N w_n U_n^M - \sum_{n=0}^N w_n U_n^0.$$

Therefore,

$$\Delta x \left(\sum_{n=0}^N w_n U_n^M - \sum_{n=0}^N w_n U_n^0 \right) = -(\Delta t) I^D \left[\sum_{m=0}^M F(U(1, t_m)) - \sum_{m=0}^M F(U(-1, t_m)) \right], \quad (11)$$

and if $\Delta x, \Delta t \rightarrow 0$ then (11) approaches the integral form of the conservation law (8).

4.2 One-dimensional systems of conservation laws ($c > 1, d = 1$)

If $u(x, t) = (u_1(x, t), \dots, u_c(x, t))^T$ and $F(u) = (F_1(u), \dots, F_c(u))^T$, then (1) becomes

$$\begin{pmatrix} u_1 \\ \vdots \\ u_c \end{pmatrix}_t + \begin{pmatrix} F_1(u) \\ \vdots \\ F_c(u) \end{pmatrix}_x = \begin{pmatrix} 0 \\ \vdots \\ 0 \end{pmatrix},$$

with initial conditions $u_i(x, 0) = u_i^0(x), \forall i \in I$.

Its mimetic scheme, for a forward Euler discretization in time t_m , is

$$\frac{1}{\Delta t} (U_i^{m+1} - U_i^m) = -DI^D F_i(U^m), \quad \forall i \in I,$$

Multiplying by $\mathbf{1}^T Q$ on the left, one obtains,

$$\frac{1}{\Delta t} \mathbf{1}^T Q (U_i^{m+1} - U_i^m) = -\frac{1}{\Delta x} I^D (F_i(u(1, t_m)) - F_i(u(-1, t_m))), \quad i \in I,$$

or equivalently,

$$\frac{\Delta x}{\Delta t} \begin{pmatrix} \sum_{n=0}^N w_n (U_1(x_n, t_{m+1}) - U_1(x_n, t_m)) \\ \vdots \\ \sum_{n=0}^N w_n (U_c(x_n, t_{m+1}) - U_c(x_n, t_m)) \end{pmatrix} = -I^D \begin{pmatrix} F_1(U(1, t_m)) - F_1(U(-1, t_m)) \\ \vdots \\ F_c(U(1, t_m)) - F_c(U(-1, t_m)) \end{pmatrix}. \quad (12)$$

For periodic boundary conditions, (12) implies,

$$\Delta x \sum_{n=0}^N w_n U_i(x_n, t_{m+1}) = \Delta x \sum_{n=0}^N w_n U_i(x_n, t_m) = \dots = \Delta x \sum_{n=0}^N w_n U_i(x_n, 0), \quad \forall i \in I,$$

and this reflects the conservation at the discrete level, since $\Delta x \sum_{n=0}^N w_n U_i(x_n, 0)$ is a high-order approximation of $\int_{-1}^1 u_i^0(x) dx, \forall i \in I$.

For non-periodic boundary conditions, sum (12) from $m = 0$ to $m = M$, and utilizing the telescoping property implies

$$(\Delta x) \begin{pmatrix} \sum_{n=0}^N w_n(U_1(x_n, T) - U_1(x_n, 0)) \\ \vdots \\ \sum_{n=0}^N w_n(U_c(x_n, T) - U_c(x_n, 0)) \end{pmatrix} = -(\Delta t) I^D \begin{bmatrix} \sum_{m=0}^M (F_1(U(1, t_m)) - F_1(U(-1, t_m))) \\ \vdots \\ \sum_{m=0}^M (F_c(U(1, t_m)) - F_c(U(-1, t_m))) \end{bmatrix},$$

and if $\Delta x, \Delta t \rightarrow 0$ then the integral form of the conservation law is obtained.

4.3 Systems of conservation laws of arbitrary dimensions ($c, d > 1$)

If $x = (x_1, \dots, x_d)$, $u(x, t) = (u_1(x, t), \dots, u_c(x, t))^T$ and $F(u) = (F_1(u), \dots, F_c(u))^T$, then (1) becomes

$$\begin{pmatrix} u_1 \\ \vdots \\ u_c \end{pmatrix}_t = - \begin{pmatrix} \sum_{j=1}^d (F_{1j})_{x_j} \\ \vdots \\ \sum_{j=1}^d (F_{cj})_{x_j} \end{pmatrix},$$

with initial conditions $u_i(x, 0) = u_i^0(x)$, $\forall i \in I$.

If one uses a lexicographic ordering in d -dimensions and U_i stands for U_i at all points in X_C accordingly, then for any fixed $i \in I$, its mimetic scheme can be written as

$$\frac{1}{\Delta t} (U_i^{m+1} - U_i^m) = -D_{x_1 \dots x_d} I_{x_1 \dots x_d}^D F_i(U^m), \quad \forall i \in I.$$

Multiplying by $(\prod_{j=1}^d \Delta x_j) \mathbb{1}^T Q_{x_1 \dots x_d}$ on the left, one obtains using (6) that

$$\begin{aligned} \left(\prod_{j=1}^d \Delta x_j \right) \mathbb{1}^T Q_{x_1 \dots x_d} (U_i^{m+1} - U_i^m) &= -\Delta t \left(\prod_{j=1}^d \Delta x_j \right) \mathbb{1}^T Q_{x_1 \dots x_d} D_{x_1 \dots x_d} I_{x_1 \dots x_d}^D F_i(U^m) \\ &= -\Delta t I_{x_1 \dots x_d}^D \sum_{l=1}^d (F_{il}(u(x_l^+, t_m)) - F_{il}(u(x_l^-, t_m))), \end{aligned} \tag{13}$$

where $x_l^\pm = (x_1, \dots, x_{l-1}, \pm 1, x_{l+1}, \dots, x_d)$.

The left hand side of (13) is the difference of discrete mass \mathcal{M}_i^{m+1} of U_i at time t_{m+1} and the discrete mass \mathcal{M}_i^m at time t_m . If the positive diagonal matrix $Q_{x_1 \dots x_d} = \text{diag}(w_{n_1, \dots, n_d})$

then (13) can be written as

$$\begin{pmatrix} \mathcal{M}_1^{m+1} - \mathcal{M}_1^m \\ \vdots \\ \mathcal{M}_c^{m+1} - \mathcal{M}_c^m \end{pmatrix} = -\Delta t I_{x_1 \dots x_d}^D \begin{pmatrix} \sum_{l=1}^d (F_{1l}(U(x_l^+, t_m) - F_{1l}(U(x_l^-, t_m)))) \\ \vdots \\ \sum_{l=1}^d (F_{cl}(U(x_l^+, t_m) - F_{cl}(U(x_l^-, t_m)))) \end{pmatrix}. \quad (14)$$

For periodic boundary conditions, (14) implies,

$$\mathcal{M}_i^{m+1} = \mathcal{M}_i^m = \dots = \mathcal{M}_i^1 = \mathcal{M}_i^0,$$

and this reflects the conservation at the discrete level, since M_i^0 is a high-order approximation of $\int_L u_i^0(x) dx$, $\forall i \in I$.

For non-periodic boundary conditions, sum (14) from $m = 0$ to $m = M$, and utilizing the telescoping property implies

$$\begin{pmatrix} \mathcal{M}_1^M - \mathcal{M}_1^0 \\ \vdots \\ \mathcal{M}_c^M - \mathcal{M}_c^0 \end{pmatrix} = -(\Delta t) I_{x_1 \dots x_d}^D \begin{pmatrix} \sum_{m=0}^M \sum_{l=1}^d (F_{1l}(U(x_l^+, t_m) - F_{1l}(U(x_l^-, t_m)))) \\ \vdots \\ \sum_{m=0}^M \sum_{l=1}^d (F_{cl}(U(x_l^+, t_m) - F_{cl}(U(x_l^-, t_m)))) \end{pmatrix},$$

and if $\Delta x_1, \dots, \Delta x_d, \Delta t \rightarrow 0$ then the integral form of the conservation law is obtained.

5 Mimetic schemes energy preservation for conservation laws

In this section the preservation of energy of mimetic schemes is shown. Even though one can split the proofs in three different cases, as in the case of mass preservation, we utilize the formula of the divergence of a product of a scalar and a vector field to exhibit the preservation of 1D scalar and systems of conservation laws and then the general case. It turns out that the approach followed for the one-dimension cases, does not work in several dimensions systems of conservation laws due to the presence of both gradient and divergence differential operators. In that case, one requires the utilization of the fact that both one-dimensional P and Q are quadratures for general functions. A mimetic scheme is proposed and it is demonstrated that when $\Delta x_1, \dots, \Delta x_d, \Delta t \rightarrow 0$ the scheme preserves energy in the sense that it approaches the integral formulation of the general system of conservation laws.

5.1 One-dimensional scalar conservation law ($c = 1, d = 1$)

Consider

$$u_t = -(F(u))_x.$$

If one multiplies by u , one gets

$$\frac{1}{2} \frac{d(u^2)}{dt} = -u(F(u))_x = u_x F(u) - (u F(u))_x,$$

where the product rule of spatial differentiation has been applied. Assuming that the discrete projection of $u(x, t)$, at any fixed t is defined at X_C by

$$U_n(t) = (U(x_0, t_n), U(x_{\frac{1}{2}}, t_n), \dots, U(x_{N-\frac{1}{2}}, t_n), U(x_N, t_n))^T,$$

then the mimetic difference discrete analog scheme is

$$\frac{1}{2 \Delta t} (U_{n+1}^2 - U_n^2) = DI^D \text{diag}(U) F(U) - DI^D H(U),$$

where $H(U(x_i, t)) = U(x_i, t) F(U(x_i, t))$, $x_i \in X_C$, and I^D is the interpolation operator from centers X_C to nodes X_F . Therefore,

$$\frac{\Delta x}{2 \Delta t} \mathbf{1}^T Q (U_{n+1}^2 - U_n^2) = (\Delta x) [\mathbf{1}^T Q D \{I^D \text{diag}(U) F(U) - I^D H(U)\}],$$

and since Q is actually a high-order quadrature, i.e., $(\Delta x) \mathbf{1}^T Q W$ is a high-order approximation of $\int_{-1}^1 W(x) dx$, then

$$\begin{aligned} \frac{1}{2} (\mathcal{E}(U_{n+1}) - \mathcal{E}(U_n)) &= \Delta t (-1, 0, \dots, 0, 1) (I^D \text{diag}(U) F(U) - I^D H(U)) \\ &= \Delta t I^D (\text{diag}(U(1, t_n)) F(U(1, t_n)) - H(U(x(1, t_n)))) \\ &\quad - \Delta t I^D (\text{diag}(U(-1, t_n)) F(U(-1, t_n)) - H(U(x(-1, t_n)))) = 0, \end{aligned}$$

where the left term comes from a definition of discrete energy, i.e., $\mathcal{E}(U) = (\Delta x) \mathbf{1}^T Q U^2$, the first identity comes from (5) and the last one from the definition of $H(U)$.

Hence, the discrete energy is preserved at every time step.

5.2 One-dimensional systems of conservation laws ($c > 1, d = 1$)

If $u(x, t) = (u_1(x, t), \dots, u_c(x, t))^T$ and $F(u) = (F_1(u), \dots, F_c(u))^T$, then (1) becomes

$$\frac{du_i}{dt} = -(F_i(u))_x, \quad i \in I,$$

with initial conditions $u_i(x, 0) = u_i^0(x), \forall i \in I$.

If one multiplies the i -th equation, $i \in I$, by u_i and applies the product rule differentiation, one obtains

$$\frac{1}{2} \frac{d(u_i^2)}{dt} = -u_i (F(u))_x = \frac{du_i}{dx} F(u) - (u_i F(u))_x, \quad i \in I,$$

whose mimetic difference discrete analog scheme, utilizing a forward Euler time discretization, is

$$\frac{1}{2\Delta t} (U_{n+1}^2 - U_n^2) = DI^D \text{diag}(U_i) F(U) - DI^D H_i(U), \quad i \in I,$$

where $H_i(U(x_j, t)) = U_i(x_j, t) F(U(x_j, t))$, $x_j \in X_C$, and I^D is the interpolation operator from centers X_C to nodes X_F . Therefore, multiplying on the left by $(\Delta x) \mathbf{1}^T Q$, one gets

$$\frac{\Delta x}{2} \mathbf{1}^T Q (U_{n+1}^2 - U_n^2) = \Delta t (\Delta x \mathbf{1}^T Q D) (I^D \text{diag}(U_i) F(U) - I^D H_i(U)), \quad i \in I,$$

and from the discrete energy definition, one gets for a fixed $i \in I$,

$$\begin{aligned} \frac{1}{2} (\mathcal{E}(U_{n+1}) - \mathcal{E}(U_n)) &= \Delta t (-1, 0, \dots, 0, 1) (I^D \text{diag}(U_i) F(U) - I^D H_i(U)) \\ &= \Delta t I^D (\text{diag}(U_i(1, t_n)) F(U(1, t_n)) - H_i(U(x(1, t_n)))) \\ &\quad - \Delta t I^D (\text{diag}(U_i(-1, t_n)) F(U(-1, t_n)) - H_i(U(x(-1, t_n)))) = 0, \end{aligned}$$

where the last identity comes from the definition of $H_i(U)$, $i \in I$.

5.3 Systems of conservation laws of arbitrary dimensions ($c, d > 1$)

If $x = (x_1, \dots, x_d)$, $u(x, t) = (u_1(x, t), \dots, u_c(x, t))^T$ and $F(u) = (F_1(u), \dots, F_c(u))^T$, then (1) becomes

$$\begin{pmatrix} u_1 \\ \vdots \\ u_c \end{pmatrix}_t = - \begin{pmatrix} \sum_{j=1}^d (F_{1j})_{x_j} \\ \vdots \\ \sum_{j=1}^d (F_{cj})_{x_j} \end{pmatrix},$$

and if one multiplies the i -th equation $i \in I$, by u_i one gets

$$\frac{1}{2} \frac{du_i^2}{dt} = -u_i \sum_{j=1}^d (F_{ij})_{x_j} = F_i \cdot \text{grad}(u_i) - \text{div}(u_i F_i), \quad (15)$$

and the corresponding mimetic scheme is

$$\frac{1}{2 \Delta t} ((U_i^{m+1})^2 - (U_i^m)^2) = \text{diag}(F_i(U)) I^G G U_i - D_{x_1, \dots, x_d} H_i(U),$$

where $H_i(U) = U_i F_i(U)$.

The presence of the both G and D in the right hand side of the previous identity complicates matters if one pursues to proceed in the same way as before. Ideally, one would like to change the G operator by D but the discrete analog of the integration by parts formula also includes weights P and Q . These two inner weights are identity matrices for the case of second-order accuracy ($k = 2$), but even in that case, the presence of $F_i(U)$ and U_i in the gradient term makes impossible to utilize the same approach as before. Fortunately, both P and Q are quadratures and that allows a new approach.

Another way of writing the discrete analog of (15) is

$$\frac{1}{2 \Delta t} ((U_i^{m+1})^2 - (U_i^m)^2) = \sum_{j=1}^d G_{x_1 \dots x_d, j} U_i I_{x_1 \dots x_d, j}^D F_{ij} - \sum_{j=1}^d D_{x_1 \dots x_d, j} H_{ij}(U).$$

Therefore,

$$\begin{aligned} \frac{1}{2 \Delta t} \left(\prod_{j=1}^d \Delta x_j \right) \mathbb{1}^T ((U_i^{m+1})^2 - (U_i^m)^2) &= \sum_{j=1}^d \left(\prod_{j=1}^d \Delta x_j \right) \mathbb{1}^T G_{x_1 \dots x_d, j} U_i I_{x_1 \dots x_d, j}^D F_{ij} \\ &- \sum_{j=1}^d \left(\prod_{j=1}^d \Delta x_j \right) \mathbb{1}^T D_{x_1 \dots x_d, j} H_{ij}(U), \end{aligned}$$

and since each component of G and D are one-dimensional quadratures one gets, for $\Delta x_1, \dots, \Delta x_d$ small, that

$$\begin{aligned}
& \frac{1}{2\Delta t} \left(\prod_{j=1}^d \Delta x_j \right) \mathbf{1}^T ((U_i^{m+1})^2 - (U_i^m)^2) = \\
& \sum_{j=1}^d [U_i(x_1, \dots, x_{j-1}, 1, x_{j+1}, \dots, x_d) I_{x_1 \dots x_d, j}^D F_{ij}(x_1, \dots, x_{j-1}, 1, x_{j+1}, \dots, x_d) - \\
& U_i(x_1, \dots, x_{j-1}, -1, x_{j+1}, \dots, x_d) I_{x_1 \dots x_d, j}^D F_{ij}(x_1, \dots, x_{j-1}, -1, x_{j+1}, \dots, x_d)] - \\
& \sum_{j=1}^d (H_{ij}(x_1, \dots, x_{j-1}, 1, x_{j+1}, \dots, x_d) - H_{ij}(x_1, \dots, x_{j-1}, -1, x_{j+1}, \dots, x_d)) = 0,
\end{aligned}$$

because of the definition of H_i . Hence,

$$\mathbf{1}^T (U_i^{m+1})^2 = \mathbf{1}^T (U_i^m)^2,$$

which shows energy preservation of the scheme if one uses the discrete standard energy definition.

6 Numerics

Two examples are considered. The first example refers to a 1D linear conservation law. The second one introduces a two-dimensional system of four conservation laws.

6.1 One-dimensional advection equation

Consider the one-dimensional advection equation [18, p. 2546].

$$\frac{\partial \psi}{\partial t} + U \frac{\partial \psi}{\partial x} = 0, \tag{16}$$

where velocity $U = 10 \text{ ms}^{-1}$ is constant in a periodic domain $-8 \leq x \leq 8 \text{ km}$ using a grid spacing of $\Delta x = 100 \text{ m}$. The initial position is given by $\psi_0(x) = \cos(\frac{2\pi x}{l}) \exp(-\frac{x^2}{d^2})$, where $d = 4 \text{ km}$ and $l = 2.5 \text{ km}$. Equation (16) is numerically integrated utilizing the fifth-order filtered leapfrog (LF-MMK) with $\gamma_6 = 0.1$ time discretization, which is second-order accurate. Three choices of time steps Δt such that the corresponding Courant numbers $\mu = \frac{U\Delta t}{\Delta x}$ are 0.2, 0.4 and 0.6. Spatial derivatives are approximated by fourth-order Corbino-Castillo mimetic method, and the total number of time steps is chosen so that the initial perturbation is transported one revolution around the domain.

The fifth-order LF-MMK needs initial data to be able to start. This initial data is obtained by performing a half-step forward Euler followed by three leapfrog steps.

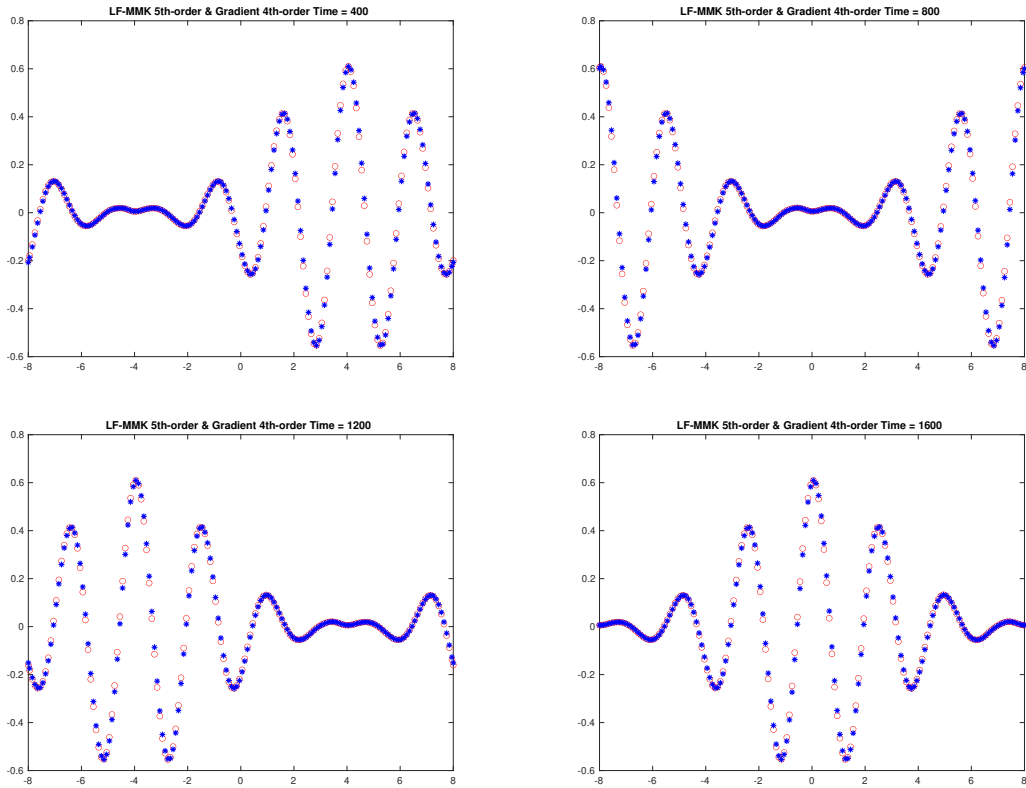


Figure 1: The numerical solution of the 3D advection equation utilizing the fifth-order LF-MMK scheme. The initial condition is displayed on the right lower panel. Some plots of the numerical solution are shown on the left upper (400 s), right upper (800 s), left lower (1200 s), and right lower (1600 s) panels.

In Figure 1 one can see the evolution and the level of accuracy of the numerical solution of the fifth-order LF-MMK time scheme together with the fourth-order Corbino-Castillo mimetic difference at 400s, 800s, 1200s, 1600s, respectively. It is clear that mass is preserved along the time integration.

In addition, the total energy of the solution of the advection equation with constant velocity should be also constant. Utilizing the fifth-order LF-MMK time scheme (of second order accuracy in time) together with the fourth-order Corbino-Castillo mimetic difference operator at each time step is exhibited in Figure 2. Observe it is almost constant. Only the first steps (which are obtained via a forward Euler and a leapfrog schemes) have a little different total energy.

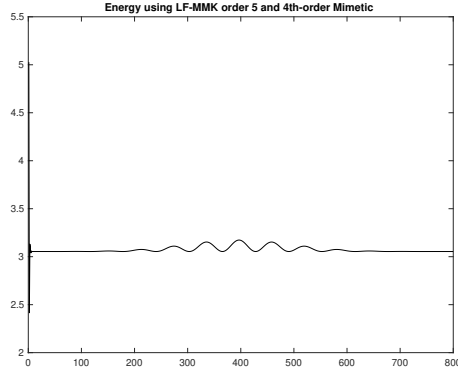


Figure 2: Total energy at each time step of the solution of the advection equation.

6.2 Two-dimensional Euler equations

The following problem has been taken from [14, pp.18-19].

Consider the 2D Euler equations

$$\frac{\partial q}{\partial t} + \nabla \cdot f = 0, \quad (17)$$

with

$$q = \begin{pmatrix} \rho \\ \rho u \\ \rho v \\ E \end{pmatrix}, \quad f_1 = \begin{pmatrix} \rho u \\ \rho u^2 + p \\ \rho u v \\ (E + p)u \end{pmatrix}, \quad f_2 = \begin{pmatrix} \rho v \\ \rho u v \\ \rho v^2 + p \\ (E + p)v \end{pmatrix},$$

where ρ is the density, u the horizontal velocity, v the vertical velocity, and E the total energy. The equations are closed by the ideal gas law

$$p = (\gamma - 1) \left(E - \frac{1}{2} \rho(u^2 + v^2) \right),$$

where γ is a fluid-dependent constant, which for typical atmospheric gases can be taken to be $\gamma = \frac{7}{5}$.

For a smooth exact solution, initially centered at (x_0, y_0) and convected at the constant

velocity (u_0, v_0) , one can consider an isentropic vortex given as

$$\begin{aligned}\rho &= \left(1 - \left(\frac{\gamma - 1}{16\gamma\pi^2}\right) \beta^2 e^{2(1-r^2)}\right)^{\frac{1}{\gamma-1}}, \\ u &= u_0 - \beta e^{(1-r^2)} \frac{y - y_0}{2\pi}, \\ v &= v_0 + \beta e^{(1-r^2)} \frac{x - x_0}{2\pi}, \\ p &= \rho^\gamma,\end{aligned}$$

or equivalently

$$E = \frac{\rho^\gamma}{\gamma - 1} + \frac{1}{2}\rho(u^2 + v^2),$$

where

$$r = \sqrt{(x - u_0 t - x_0)^2 + (y - v_0 t - y_0)^2}.$$

Assume a $[-5, 5] \times [-5, 5]$ 2D domain, with $\beta = 5.0$, and the initial position of the vortex and the initial convection velocity given by

$$x_0 = y_0 = 0, u_0 = 1, v_0 = 0.$$

We employed Corbino-Castillo fourth-order mimetic operators in conjunction with a second-order leapfrog scheme for the temporal discretization to resolve (17). The visual representation of our findings is illustrated in Figures 3 through 6, presenting the approximated solutions for the conserved quantities $(\rho, \rho u, \rho v, E)$ after 0.1 seconds. Figure 7 portrays the variation of each quantity over time. This is obtained by numerically integrating the solution surfaces at various stages.

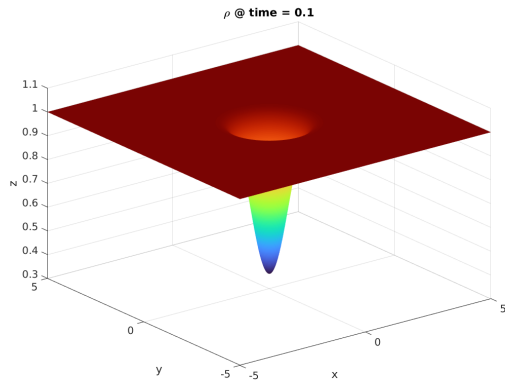


Figure 3: Density profile after 0.1 seconds.

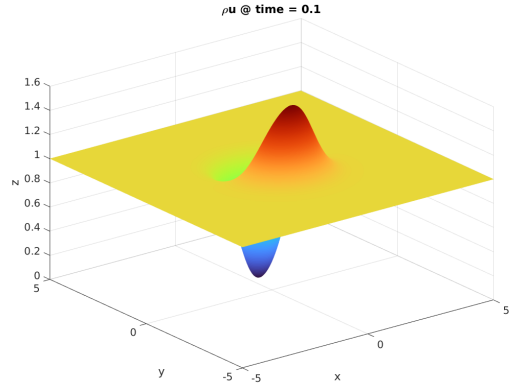


Figure 4: Momentum in the u -direction.

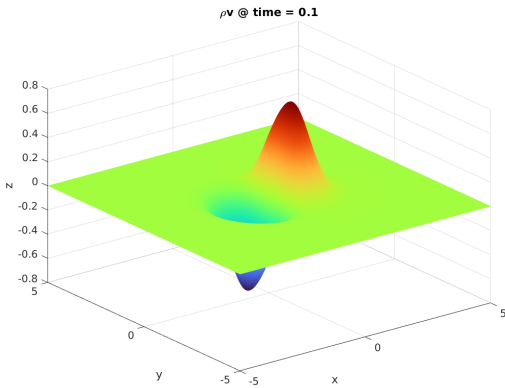


Figure 5: Momentum in the v -direction.

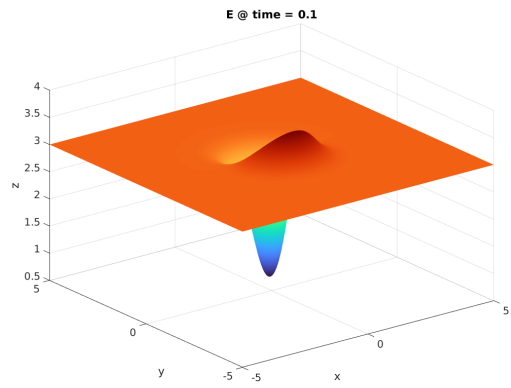


Figure 6: Total energy after 0.1 seconds.

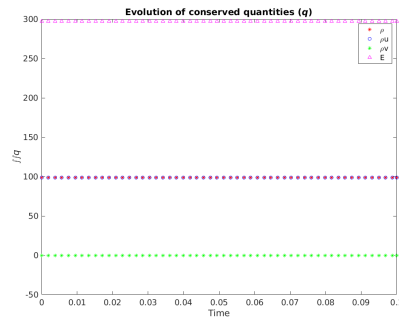


Figure 7: Variability of the four quantities of interest over time.

We thanks Dr. Johnny Corbino for the implementation of this example.

7 Conclusions

This document first establishes the known properties of the different high-order mimetic difference operators before demonstrating the mass and energy preservation for systems of conservation laws. The mathematical proof relies on two properties of the inner product weight associated to the divergence discrete analog. Firstly, a relationship that comes from the enforcement of a high-order accurate approximation of the integration by parts formula and secondly, the quadrature character of these inner product weights.

In addition, the mass conservation property is numerically illustrated by the simulation of several scalar and system of conservation laws examples on one-dimension and on several dimensions.

References

- [1] Srinivasan, A., Dumett, A., Paolini, C., Miranda, G.F., and Castillo, J.E., Mimetic finite difference operators and higher order quadratures, *Int. J. Geomath* 14 (19), 2023, <https://doi.org/10.1007/s13137-023-00230-z>.
- [2] Arnold, D.N., *Finite Element Exterior Calculus*, SIAM, 2018.
- [3] J.E. Castillo and R.D. Grone, A Matrix Analysis Approach to Higher-Order Approximations for Divergence and Gradients Satisfying a Global Conservation Law, *SIAM J. Matrix Anal. Appl.*, Vol. 25, No. 1, pp. 128-142, 2003.
- [4] J. Corbino, and J.E. Castillo, High-order mimetic finite-difference operators satisfying the extended Gauss divergence theorem, *J. Comput. Appl. Math.*, v. 364, 2020.
- [5] da Veiga, L.B., Lipnikov, K., and Manzini, G., *The mimetic finite difference method for elliptic problems*, Springer, 2014.
- [6] Dumett, M.A., and Castillo, J.E., Gradient and Divergence Corbino-Castillo Interpolation Operators, San Diego State University, CSRC Report, 5-Dec-2022.
- [7] Dumett, M.A., and Castillo, J.E., Energy Conservation of Second-Order Mimetic Difference Schemes for the 1D Advection Equation, San Diego State University, CSRC Report, 7-Dec-2022.
- [8] Dumett, M.A., and Castillo, J.E., Mimetic Differences Vector Calculus Identities, San Diego State University, CSRC Report, 13-Jul-2023.

- [9] Dumett, M.A., and Castillo, J.E., Energy conservation and convergence of high-order mimetic schemes for the 3D advection equation, San Diego State University, CSRC Report, 21-Jul-2023.
- [10] Dumett, M.A., Corbino, J., and Castillo, J.E., Energy Preservation of High-Order Mimetic Differences for Systems of Conservation Laws, San Diego State University, CSRC Report, 27-Dec-2023.
- [11] Eldred, C., and Salinger, A., Structure-preserving numerical discretizations for domains with boundaries, Sandia National Laboratories, SAND2021-11517, <https://doi.org/10.2172/1820697>, September 2021.
- [12] Eldred, C., and Stewart, J., Differential geometric approaches to momentum-based formulations for fluids, Sandia National Laboratories, SAND2022-12945, <https://doi.org/10.2172/189006>, September 2022.
- [13] Evans, L.C., Partial Differential Equations, Graduate Studies in Mathematics, Vol. 19, American Mathematical Society, Providence, Rhode Island, 1998.
- [14] Hesthaven, J.S., Numerical methods for conservation laws, SIAM Computational Science and Engineering, Philadelphia, Pennsylvania, 2018.
- [15] Hirani, A.H., Discrete Exterior Calculus, California Institute of Technology, PhD dissertation, 2003.
- [16] Justo, D., High Order Mimetic Methods, VDM Verlag Dr. Müller Aktiengesellschaft & Co. KG, 2009.
- [17] Kreeft, J., Palha, A., and Gerritsma, M., Mimetic Framework On Curvilinear Quadrilaterals Of Arbitrary Order, arXiv:1111.4304v1 [math.NA], 2011, <https://doi.org/10.48550/arXiv.1111.4304>.
- [18] M. Moustou, A. Mahalov, and E.J. Kostelich, A Numerical Method Based on Leapfrog and a Fourth-Order Implicit Time Filter, Mon. Wea. Rev., American Meteorological Society, 2014, Vol. 142, pp. 2545-2560.
- [19] Robidoux, N. and Steinberg, S., A Discrete Vector Calculus in Tensor Grids, Computational Methods in Applied Mathematics, 11(1), pp 23-66, 2011, <https://doi.org/10.2478/cmam-2011-0002>.
- [20] Sharma, H., Patil, M., and Woolsey, C., A review of structure-preserving numerical methods for engineering applications, Computer Methods in Applied Mechanics and Engineering, Vol. 366, 113067, 1 July 2020, <https://doi.org/10.1016/j.cma.2020.113067>.
- [21] Shaskov, M., Conservative Finite-Difference Methods on General Grids, CRC Press, Boca Raton, FL, 1995.